

RESTRICTED ADDITIVE SCHWARZ PRECONDITIONERS WITH HARMONIC OVERLAP FOR SYMMETRIC POSITIVE DEFINITE LINEAR SYSTEMS

XIAO-CHUAN CAI*, MAKSYMILIAN DRYJA†, AND MARCUS SARKIS‡

Abstract. A restricted additive Schwarz (RAS) preconditioning technique was introduced recently for solving general nonsymmetric sparse linear systems. In this paper, we provide one-level and two-level extensions of RAS for symmetric positive definite problems using the so-called harmonic overlaps (RASHO). Both RAS and RASHO outperform their counterparts of the classical additive Schwarz variants (AS). The design of RASHO is based on a much deeper understanding of the behavior of Schwarz type methods in overlapping subregions, and in the construction of the overlap. In RASHO, the overlap is obtained by extending the nonoverlapping subdomains only in the directions that do not cut the boundaries of other subdomains, and all functions are made harmonic in the overlapping regions. As a result, the subdomain problems in RASHO are smaller than that of AS, and the communication cost is also smaller when implemented on distributed memory computers, since the right-hand sides of discrete harmonic systems are always zero that do not need to be communicated. We also show numerically that RASHO preconditioned CG takes fewer number of iterations than the corresponding AS preconditioned CG. A nearly optimal theory is included for the convergence of RASHO preconditioned CG for solving elliptic problems discretized with a finite element method.

Key words. Restricted additive Schwarz preconditioner, two-level domain decomposition, harmonic overlap, elliptic equations, finite elements

AMS subject classifications. 65N30, 65F10

1. Introduction. A restricted additive Schwarz (RAS) preconditioning technique was introduced recently for solving general nonsymmetric sparse linear systems [1, 5, 7, 14, 16, 17, 20]. RAS outperforms the classical additive Schwarz preconditioner (AS) [8, 24] in the sense that it requires fewer number of iterations, as well as smaller communication and CPU time costs when implemented on distributed memory computers, [1]. Unfortunately, RAS in its original form is nonsymmetric and therefore the conjugate gradient method (CG) cannot be used [15]. Although a symmetrized version was constructed in [7], our numerical experiments show that it often takes more iterations than the corresponding AS/CG. In this paper we propose another modification of RAS and show in both theory and numerical experiments that this new variant works well for symmetric positive definite sparse linear systems and is superior to AS. Recall that the basic building blocks of classical Schwarz type algorithms are realized by solving the linear systems of the form

$$(1.1) \quad A_i^\delta w = R_i^\delta v$$

on each extended subdomain, where A_i^δ is the extended subdomain stiffness matrix and R_i^δ is the restriction operator for the extended subdomain (formal definitions will

*Department of Computer Science, University of Colorado, Boulder, CO 80309, (cai@cs.colorado.edu). The work was supported in part by the NSF grants ACI-0072089, ACI-0083004, and ACI-0112930.

†Faculty of Mathematics, Informatics and Mechanics, Warsaw University, Warsaw, (dryja@mimuw.edu.pl). This work was supported in part by the NSF grant CCR-9732208 and in part by the Polish Science Foundation grant 2 P03A 021 16.

‡Mathematical Sciences Department, Worcester Polytechnic Institute, Worcester, MA 01609, (msarkis@wpi.edu) and Instituto de Matemática Pura e Aplicada. The work was supported in part by the NSF grant CCR-9984404.

be given later in the paper). The key idea of RAS is that equation (1.1) is replaced by

$$(1.2) \quad A_i^\delta w = \begin{cases} v & \text{inside the un-extended subdomain} \\ 0 & \text{in the overlapping part of the subdomain.} \end{cases}$$

Note that the solution of (1.2) is discrete harmonic in the overlapping part of the subdomain, and therefore carries minimum energy in some sense. Setting part of the right-hand side vector to zero reduces the energy of the solution, and also destroys the symmetry of the additive Schwarz operator. In this paper, we further explore the idea of “harmonic overlap” and at the same time keep the symmetry of the Schwarz preconditioner. We mention that other approaches can also be taken to modify the Schwarz algorithm in the overlapping regions, such as allowing the functions to be discontinuous [4].

The algorithm to be discussed below is applicable for general symmetric positive definite problems. However, in order to provide a complete mathematical analysis, we restrict our discussion to a finite element problem, [3]. We consider a simple variational problem: Find $u \in H_0^1(\Omega)$, such that

$$(1.3) \quad a(u, v) = f(v), \quad \forall v \in H_0^1(\Omega),$$

where

$$a(u, v) = \int_{\Omega} \nabla u \cdot \nabla v \, dx \quad \text{and} \quad f(v) = \int_{\Omega} f v \, dx \quad \text{for} \quad f \in L^2(\Omega).$$

For simplicity, let Ω be a bounded polygonal region in \mathfrak{R}^2 with a diameter of size $O(1)$. The extension of the results to \mathfrak{R}^3 can be carried out easily by using the theory developed here in this paper and the well-known three-dimensional additive Schwarz techniques; [9, 10, 12]. Let $\mathcal{T}^h(\Omega)$ be a shape regular, quasi-uniform triangulation, of size $O(h)$, of Ω and $\mathcal{V} \subset H_0^1(\Omega)$ the finite element space consisting of continuous piecewise linear functions associated with the triangulation. We are interested in solving the following discrete problem associated with (1.3): Find $u^* \in \mathcal{V}$ such that

$$(1.4) \quad a(u^*, v) = f(v), \quad \forall v \in \mathcal{V}.$$

Using the standard basis functions, (1.4) can be rewritten as a linear system of equations

$$(1.5) \quad Au^* = f.$$

For simplicity, we understand u^* and f both as functions and vectors depending on the situation.

The paper is organized as follows. In section 2, we introduce notations. The new algorithm is described in section 3. Section 4 is devoted to the mathematical analysis of the new algorithm. We conclude the paper in section 5 by providing some numerical results and final remarks. Through out this paper, C is a positive generic constant that is independent of any of the mesh parameters and the number of subdomains. All the domains and subdomains are assumed to be open; i.e., boundaries are not included in their definitions.

2. Notations. Let n be the total number of interior nodes of $\mathcal{T}^h(\Omega)$ and W the set containing all the interior nodes. We assume that a node-based partitioning has been applied and resulted in N nonoverlapping subsets $W_i^0, i = 1, \dots, N$, whose union is W . For each W_i^0 , we define a subregion Ω_i^R as the union of all elements of $\mathcal{T}^h(\Omega)$ that have all three vertices in $W_i^0 \cup \partial\Omega$. Note that $\cup \bar{\Omega}_i^R$ is not equal to $\bar{\Omega}$; see Fig. 2.1(b). We denote by H as the representative size (diameter) of the subregion Ω_i^R .

We define the overlapping partition of W as follows. Let $\{W_i^1\}$ be the one-overlap partition of W , where $W_i^1 \supset W_i^0$ is obtained by including all the immediate neighboring vertices of all vertices in W_i^0 ; see Fig. 2.1(c). Using the idea recursively, we can define a δ -overlap partition of W ,

$$W = \bigcup_{i=1}^N W_i^\delta.$$

Here the integer δ indicates the level of overlap with its neighboring subdomains and δh is approximately the extend of the extension. The definition of W_i^δ , as well as many other subsets, can be found in an illustrative picture, Fig. 2.1.

We next define a subregion of Ω induced by a subset of nodes of $\mathcal{T}^h(\Omega)$ as follows. Let Z be a subset of W . The induced subregion, denoted as $\Omega(Z)$, is defined as the union of: (1) the set Z itself; (2) the union of all the open elements (triangles) of $\mathcal{T}^h(\Omega)$ that have at least one vertex in Z ; and (3) the union of the open edges of these triangles that have at least one endpoint as a vertex of Z . Note that $\Omega(Z)$ is always an open region. The extended subregion Ω_i^δ is defined as $\Omega(W_i^\delta)$, and the corresponding subspace as

$$\mathcal{V}_i^\delta \equiv \mathcal{V} \cap H_0^1(\Omega_i^\delta) \text{ extended by zero to } \Omega \setminus \Omega_i^\delta.$$

It is easy to verify that

$$\mathcal{V} = \mathcal{V}_1^\delta + \mathcal{V}_2^\delta + \dots + \mathcal{V}_N^\delta.$$

This decomposition is used in defining the classical one-level additive Schwarz algorithm [8]. Note that for $\delta = 0$ this decomposition is a direct sum. Let us define $P_i^\delta : \mathcal{V} \rightarrow \mathcal{V}_i^\delta$ by: for any $u \in \mathcal{V}$,

$$(2.1) \quad a(P_i^\delta u, v) = a(u, v), \quad \forall v \in \mathcal{V}_i^\delta.$$

Then, the classical one-level additive Schwarz operator has the form

$$P^\delta = P_1^\delta + \dots + P_N^\delta.$$

In the classical AS as defined above, all the nodes of W_i^δ are treated equally even through some subsets of the nodes play different roles in determining the convergence rate of the AS preconditioned CG. To further understand the issue, we classify the nodes as follows. Let $\Gamma_i^\delta = \partial\Omega_i^\delta \setminus \partial\Omega$; i.e., the part of the boundary of Ω_i^δ that does not belong to the Dirichlet part of the physical boundary $\partial\Omega$. We define the interface overlapping boundary Γ^δ as the union of all Γ_i^δ ; i.e., $\Gamma^\delta = \cup_{i=1}^N \Gamma_i^\delta$. We also need to define the following subsets of W , see, for examples, Fig. 2.1, where $\delta = 1$:

- $W^{\Gamma^\delta} \equiv W \cap \Gamma^\delta$ (interface nodes)

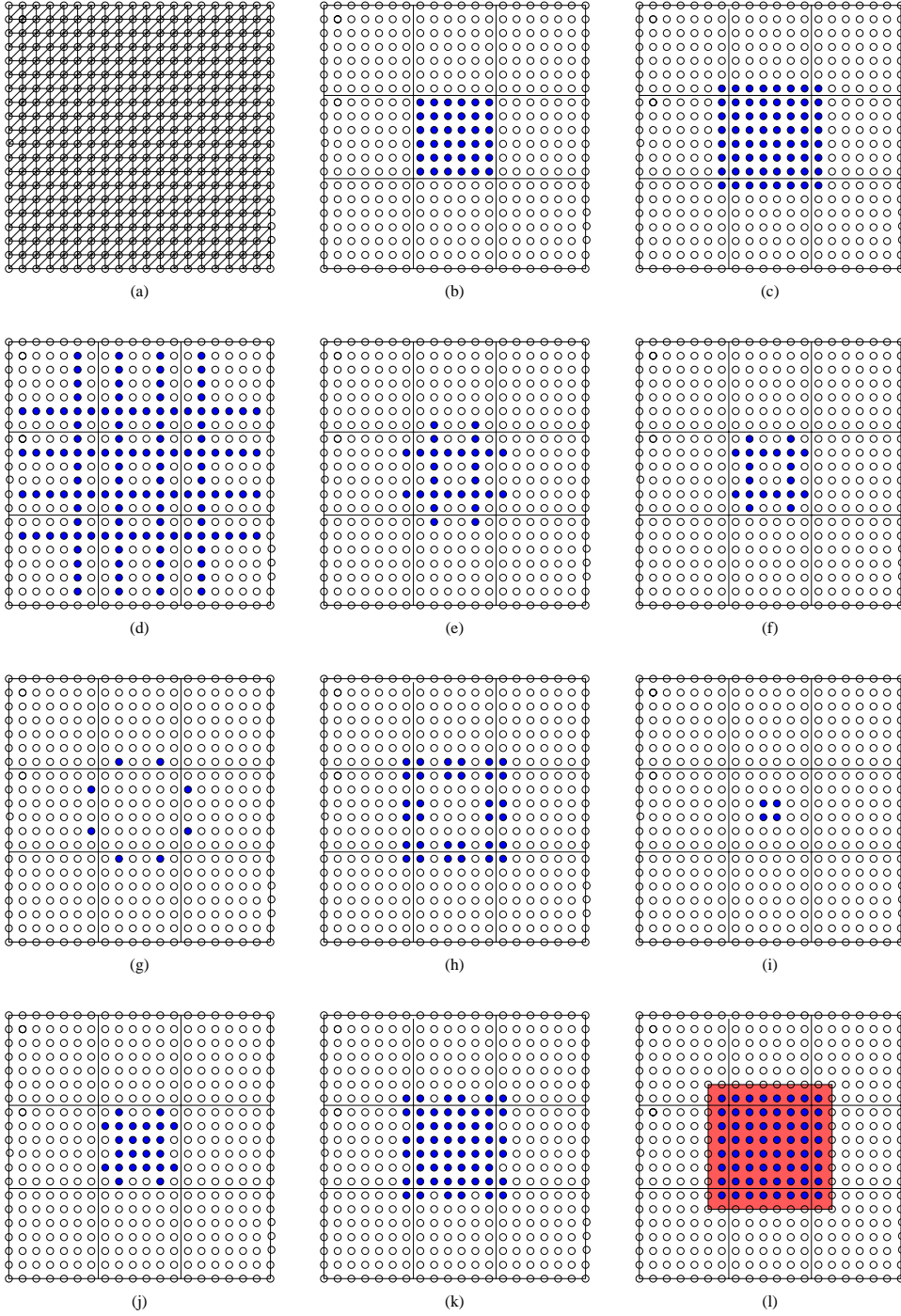


FIG. 2.1. The partition of a finite element mesh into 9 subdomains with the overlapping factor $\delta = 1$. (a) the finite element mesh and nodal points; (b) a node-based partition of the mesh into 9 nonoverlapping subsets, and the collection of “•” forms the set W_i^0 ; (c) W_i^δ ; (d) $W_i^{\Gamma^\delta}$; (e) $W_i^{\Gamma^\delta}$; (f) $W_{i,in}^{\Gamma^\delta}$; (g) $W_{i,cut}^{\Gamma^\delta}$; (h) $W_{i,ovl}^\delta$; (i) $W_{i,non}^\delta$; (j) $W_{i,in}^\delta$; (k) \tilde{W}_i^δ ; (l) the shadowed area is Ω_i^δ .

- $W_i^{\Gamma^\delta} \equiv W^{\Gamma^\delta} \cap W_i^\delta$ (local interface nodes)
- $W_{i,in}^{\Gamma^\delta} \equiv W^{\Gamma^\delta} \cap W_i^0$ (local internal interface nodes)
- $W_{i,cut}^{\Gamma^\delta} \equiv W_i^{\Gamma^\delta} \setminus W_{i,in}^{\Gamma^\delta}$ (local cut interface nodes)
- $W_{i,ovl}^\delta \equiv (W_i^\delta \setminus W_i^{\Gamma^\delta}) \cap (\bigcup_{j \neq i} W_j^\delta)$ (local overlapping nodes)
- $W_{i,non}^\delta \equiv W_i^\delta \setminus (W_i^{\Gamma^\delta} \cup W_{i,ovl}^\delta)$ (local nonoverlapping nodes)
- $W_{i,in}^\delta \equiv W_{i,non}^\delta \cup W_{i,in}^{\Gamma^\delta}$ (internal nodes)

We note that the most northwest and the southeast nodes in (c) were added in Fig. 2.1 to Ω_i^δ in order to make Ω_i^δ a rectangle. This just to simplify the presentation and it is not required in the implementation of the algorithms.

We frequently use functions that are discrete harmonic at certain nodes. Let $x_k \in W$ be a mesh point and $\phi_{x_k}(x) \in \mathcal{V}$ the finite element basis function associated with x_k ; i.e., $\phi_{x_k}(x_k) = 1$, and $\phi_{x_k}(x_j) = 0$, $j \neq k$. We say $u \in \mathcal{V}$ is discrete harmonic at x_k if

$$a(u, \phi_{x_k}) = 0.$$

If u is discrete harmonic at a set of nodal points Z , we say u is discrete harmonic in $\Omega(Z)$.

Our new algorithm will be built on the subspace $\tilde{\mathcal{V}}_i^\delta$ defined as a subspace of \mathcal{V}_i^δ . $\tilde{\mathcal{V}}_i^\delta$ consists of all functions that vanish on the cutting nodes $W_{i,cut}^{\Gamma^\delta}$ and are discrete harmonic at the nodes of $W_{i,ovl}^\delta$. Note that the degrees of freedom associated to the subspace $\tilde{\mathcal{V}}_i^\delta$ is

$$\tilde{W}_i^\delta \equiv W_i^\delta \setminus W_{i,cut}^{\Gamma^\delta}$$

and, since the values at the harmonic nodes are not independent, they can not be counted toward the degree of freedoms. The dimension of $\tilde{\mathcal{V}}_i^\delta$ is

$$\dim(\tilde{\mathcal{V}}_i^\delta) = |W_{i,in}^\delta|.$$

Let $\Omega(\tilde{W}_i^\delta)$ be the induced domain. It is easy to see that $\Omega(\tilde{W}_i^\delta)$ is the same as Ω_i^δ but with cuts. We denote $\Omega(\tilde{W}_i^\delta)$ by $\tilde{\Omega}_i^\delta$. We have then $\tilde{\mathcal{V}}_i^\delta = \mathcal{V} \cap H_0^1(\tilde{\Omega}_i^\delta)$ and are discrete harmonic on $\Omega(W_{i,ovl}^\delta)$. We denote $\Omega(W_{i,ovl}^\delta)$ by $\Omega_{i,ovl}^\delta$.

We define $\tilde{\mathcal{V}}^\delta \subset \mathcal{V}^\delta$ as

$$\tilde{\mathcal{V}}^\delta = \tilde{\mathcal{V}}_1^\delta \oplus \cdots \oplus \tilde{\mathcal{V}}_N^\delta,$$

which is a direct sum. We remark that functions in $\tilde{\mathcal{V}}^\delta$ are, by definition, the sum of functions $u_i \in \tilde{\mathcal{V}}_i^\delta$, $i = 1, \dots, N$. Functions in $\tilde{\mathcal{V}}^\delta$ can, in fact, be characterized easily as in the following lemma.

Lemma 2.1. *If $u \in \mathcal{V}$ and u is discrete harmonic at all the overlapping nodes, i.e., on $\bigcup_{i=1}^N W_{i,ovl}^\delta$, then $u \in \tilde{\mathcal{V}}^\delta$.*

Proof. To prove that $u \in \tilde{\mathcal{V}}^\delta$, all we need is to find a decomposition

$$u = \sum_{i=1}^N u_i, \quad \text{with } u_i \in \tilde{\mathcal{V}}_i^\delta, \quad i = 1, \dots, N.$$

For the given u , we define u_i piece by piece as follows. On the nodes in $W_{i,in}^\delta$ we let $u_i = u$. On the nodes in $W_{i,cut}^\delta$ we let u_i be zero. On the nodes outside W_i^δ we set u_i to zero. We now need only to define u_i on the nodes belong to $W_{i,ovl}^\delta$. There, we extend u_i as a discrete harmonic function with boundary data given by u_i just defined. \square

3. One-level restricted additive Schwarz with harmonic overlap (RASHO) method. Using notations introduced in the previous section, we now describe a new method, namely a restricted additive Schwarz with harmonic overlap.

We first define $\tilde{P}_i^\delta : \tilde{\mathcal{V}}^\delta \rightarrow \tilde{\mathcal{V}}_i^\delta$ as a projection operator, such that, for any $u \in \tilde{\mathcal{V}}^\delta$

$$(3.1) \quad a(\tilde{P}_i^\delta u, v) = a(u, v), \quad \forall v \in \tilde{\mathcal{V}}_i^\delta.$$

The RASHO operator can then be defined as

$$(3.2) \quad \tilde{P}^\delta = \tilde{P}_1^\delta + \dots + \tilde{P}_N^\delta.$$

Note, however, that the solution u^* of (1.4), see also (1.5), is not, generally speaking, in the subspace $\tilde{\mathcal{V}}^\delta$, therefore, the operator \tilde{P}^δ cannot be used to solve the linear system (1.5) directly. We will need to modify the right-hand side of the system (1.5). A reformulated (1.5) will be presented in Lemma 3.1 below. We will show that the elimination of the variables associated with the overlapping nodes is not needed in order to apply \tilde{P}^δ to any given vector $v \in \tilde{P}^\delta$.

We now introduce a matrix form of (3.2). We define the restriction operator, or a matrix, \tilde{R}_i^δ as follows. Let $v = (v_1, \dots, v_n)^T$ be a vector corresponding to the nodal values of a function $u \in \mathcal{V}$; namely for any node $x_k \in W$, $v_k = u(x_k)$. For convenience, we say “ v is defined on W ”. Its restriction on \tilde{W}_i^δ , $\tilde{R}_i^\delta v$, is defined as

$$(3.3) \quad \left(\tilde{R}_i^\delta v \right) (x_k) = \begin{cases} v_k & \text{if } x_k \in \tilde{W}_i^\delta \\ 0 & \text{otherwise.} \end{cases}$$

The matrix representation of \tilde{R}_i^δ is given by a diagonal matrix with 1 for nodal points in \tilde{W}_i^δ and zero for the remaining nodal points. We remark that, by way of definition, the operator \tilde{R}_i^δ is symmetric; i.e., $(\tilde{R}_i^\delta)^T = \tilde{R}_i^\delta$. Using this restriction operator, we define the subdomain stiffness matrix as

$$\tilde{A}_i^\delta = \tilde{R}_i^\delta A (\tilde{R}_i^\delta)^T,$$

which can also be obtained by the discretization of the original finite element problem on \tilde{W}_i^δ with zero Dirichlet data on nodes $W \setminus \tilde{W}_i^\delta$. The matrix \tilde{A}_i^δ is block diagonal with blocks corresponding to the structure of \tilde{R}_i^δ and its inverse is understood as an inverse of the nonzero block. A matrix representation of \tilde{P}_i^δ denoted also by \tilde{P}_i^δ is equal to

$$\tilde{P}_i^\delta = \left(\tilde{A}_i^\delta \right)^{-1} A$$

and

$$(3.4) \quad \tilde{P}^\delta = \left((\tilde{A}_1^\delta)^{-1} + \dots + (\tilde{A}_N^\delta)^{-1} \right) A.$$

Using the matrix notations, the next lemma shows how to modify the system (1.5) so that its solution belongs to $\tilde{\mathcal{V}}^\delta$.

Lemma 3.1. *Let u^* and f be the exact solution and the right-hand side of (1.5), and*

$$(3.5) \quad w = \sum_{i=1}^N (\tilde{A}_i^\delta)^{-1} \tilde{R}_i^0 f,$$

then, we have $\tilde{u}^* = u^* - w \in \tilde{\mathcal{V}}^\delta$, which is the solution of the modified linear system of equations

$$A\tilde{u}^* = f - Aw = \tilde{f}.$$

Proof. If we can show that

$$a(w, \phi_k) = f(\phi_k),$$

for a regular basis function associated with an arbitrary overlapping node $x_k \in W_{i,ovl}^\delta$, for some i , then we will have

$$(3.6) \quad a(u^* - w, \phi_k) = f(\phi_k) - f(\phi_k) = 0,$$

which says that $\tilde{u}^* = u^* - w$ is discrete harmonic at the overlapping node x_k . We can then use Lemma 2.1 to conclude the proof. Let us now consider

$$w_i = (\tilde{A}_i^\delta)^{-1} \tilde{R}_i^0 f,$$

which, by definition, is the same as

$$a(w_i, \phi_j) = (\phi_j, \tilde{R}_i^0 f), \quad \forall x_j \in \tilde{W}_i^\delta.$$

Here and in the rest of the proof, ϕ_j is the basis function associated with the node $x_j \in \tilde{W}_i^\delta$. Using that \tilde{R}_i^0 is symmetric and

$$(\phi_j, \tilde{R}_i^0 f) = (f, \tilde{R}_i^0 \phi_j) = a(u^*, \tilde{R}_i^0 \phi_j),$$

we get

$$(3.7) \quad a(w_i, \phi_j) = a(u^*, \tilde{R}_i^0 \phi_j).$$

Let us compute $a(w_i, \phi_k)$. Since x_k is an overlapping node, it cannot be on the boundary of $\tilde{\Omega}_i^\delta$. This leaves us with the following two cases.

Case (1): The support of $\phi_k(x)$ belongs to the exterior of $\tilde{\Omega}_i^\delta$. Since the supports of w_i and ϕ_k do not overlap, we have

$$a(w_i, \phi_k) = 0.$$

Case (2): The support of $\phi_k(x)$ belongs to the interior of $\tilde{\Omega}_i^\delta$. In this case, we have

$$a(w_i, \phi_k) = a(u^*, \tilde{R}_i^0 \phi_k).$$

Taking the sum of the above equality for $i = 1, \dots, N$,

$$a(w, \phi_k) = a\left(\sum_{i=1}^N w_i, \phi_k\right) = a\left(u^*, \sum_{i=1}^N \tilde{R}_i^0 \phi_k\right) = a(u^*, \phi_k),$$

which proves (3.6). Here the fact $\sum_{i=1}^N \tilde{R}_i^0 = I$ is used. \square

There are basically two ways to compute w in practice. Suppose that subdomain problems are solved using some LU factorization based method. One can use the same factorization of \tilde{A}_i^δ to modify the right-hand side of the system and to solve subdomain problems in the preconditioning steps, as what was suggested in Lemma 3.1. Or, one can obtain w by solving several small Dirichlet problems on each subdomain with zero Dirichlet boundary conditions in the overlapping regions $\Omega_{i,ovl}^\delta$. In both strategies, the computation can be done in parallel and no communication is needed in a distributed memory implementation. In the first approach \tilde{u}^* is discrete harmonic in $W_{i,ovl}^\delta \cup W_{i,non}^\delta$ and in the second approach \tilde{u}^* is discrete harmonic only in $W_{i,ovl}^\delta$. We note that the discrete harmonicity of \tilde{u}^* on $W_{i,non}^\delta$ is not required to the algorithms and to the corresponding theory developed in this paper.

Let $\tilde{f} = f - Aw$, then \tilde{u}^* is the solution of the following linear system of equations

$$(3.8) \quad A\tilde{u}^* = \tilde{f}.$$

Since $\tilde{u}^* \in \tilde{\mathcal{V}}^\delta$,

$$g \equiv \tilde{P}^\delta \tilde{u}^*$$

is well defined, and can be computed without knowing \tilde{u}^* by using the following relations:

$$a(\tilde{P}_i^\delta \tilde{u}^*, v) = a(\tilde{u}^*, v) = (\tilde{f}, v), \quad \forall v \in \tilde{\mathcal{V}}_i^\delta \text{ and } i = 1, \dots, N.$$

More precisely speaking, we can obtain g by solving the subdomain problems

$$a(g_i, v) = (\tilde{f}, v), \quad \forall v \in \tilde{\mathcal{V}}_i^\delta,$$

for $i = 1, \dots, N$, and taking $g = g_1 + \dots + g_N$. With such a right-hand side, we introduce a new linear system

$$(3.9) \quad \tilde{P}^\delta \tilde{u}^* = g,$$

which is equivalent to the linear system (3.8); see Theorem 5.1. The system (3.9) is a symmetric positive definite system under the usual energy inner product, and therefore, can be solved using the conjugate gradient method. RASHO has a few advantages over the classical AS preconditioner. Let us recall AS briefly. Let

$$(3.10) \quad (R_i^\delta v)(x_k) = \begin{cases} v_k & \text{if } x_k \in W_i^\delta \\ 0 & \text{otherwise.} \end{cases}$$

Then the AS operator takes the following matrix form

$$(3.11) \quad P^\delta = ((A_1^\delta)^{-1} + \cdots + (A_N^\delta)^{-1}) A$$

where $A_i^\delta = R_i^\delta A (R_i^\delta)^T$. Because of the inclusion of the cut interface nodes, the size of the matrix A_i^δ is $|W_i^\delta|$, which is slightly larger than the size of the matrix \tilde{A}_i^δ , which is $|\tilde{W}_i^\delta|$. In a distributed memory implementation, the operation $R_i^\delta v$ involves moving data from one processor to another, but the operation $\tilde{R}_i^\delta v$ does not involve any communication. More precisely speaking, in RASHO, if $u \in \tilde{\mathcal{V}}^\delta$, then it is easy to see that

$$(3.12) \quad \tilde{R}_i^\delta A u = \tilde{R}_{i,in}^\delta A u,$$

where $\tilde{R}_{i,in}^\delta$ is defined as

$$(3.13) \quad \left(\tilde{R}_{i,in}^\delta v \right) (x_k) = \begin{cases} v_k & \text{if } x_k \in W_{i,in}^\delta \\ 0 & \text{otherwise.} \end{cases}$$

Therefore, for functions in $\tilde{\mathcal{V}}^\delta$, we can rewrite \tilde{P}^δ , as in (3.4), in the following form

$$(3.14) \quad \tilde{P}^\delta = \left((\tilde{A}_1^\delta)^{-1} \tilde{R}_{1,in}^\delta + \cdots + (\tilde{A}_N^\delta)^{-1} \tilde{R}_{N,in}^\delta \right) A.$$

Although the operator (3.14) does not look like a symmetric operator, but it is indeed symmetric when applied to functions in the subspace $\tilde{\mathcal{V}}^\delta$. The form (3.12) takes the advantage of the fact that the operator $\tilde{R}_{i,in}^\delta$ is communication-free in the sense that it needs only the residual associated with nodes in $W_{i,in}^\delta \subset \Omega_i^0$.

We make some further comments on how the residual Au can be calculated in a distributed memory environment, for a given vector $u \in \tilde{\mathcal{V}}^\delta$. In a typical implementation, the matrix A is constructed and stored in the form of $\{\tilde{A}_i^\delta\}$, each processor has one or several of the subdomain matrix \tilde{A}_i^δ . Similarly u is stored in the form of $\{u_i\}$, where $u_i \in \tilde{\mathcal{V}}_i^\delta$. We note, however, that to compute the residual at nodes $W_{i,in}^{\Gamma^\delta}$ some communications are required. The processor associated with subdomain Ω_i^δ needs to obtain the local solution from the neighboring subdomains at nodes connected to $W_{i,in}^{\Gamma^\delta}$. It is important to note that the amount of communications does not depend on the size of the overlap since only one layer of nodes is required. This shows that in terms of communications, the RASHO is superior to AS and RAS.

4. Some two-level versions. Similar to other domain decomposition methods, the convergence rate of the single level method depends on the number of subdomains. To make the algorithm more scalable with respect to the number of subdomains, we next introduce two two-level versions of RASHO in this section. This includes an additive version and a hybrid version using the same coarse space.

Standard coarse spaces can not be used since they are usually not discrete harmonic in the overlapping regions. To construct a coarse subspace $\tilde{\mathcal{V}}_0$ of $\tilde{\mathcal{V}}$, we introduce the coarse basis functions $\phi^i(x)$, $i = 1, \dots, N$, based on a partition of unity [21] on the interface nodes W^{Γ^δ} . For each subdomain, we define the nodal values of $\phi^i(x) \in \tilde{\mathcal{V}}_i$ as follows:

$$(4.1) \quad \phi^i(x_k) = \begin{cases} 1 & \text{if } x_k \in W_{i,in}^{\Gamma^\delta} \\ \text{discrete harmonic} & \text{if } x_k \in W_{i,ovl}^\delta \cup W_{i,non}^\delta \\ 0 & \text{if } x_k \in W \setminus \tilde{W}_i^\delta. \end{cases}$$

Let us denote $\Omega(W_{i,non}^\delta)$ by $\Omega_{i,non}^\delta$. Then $\phi^i(x_k) = 1$ at $x_k \in W_{i,non}^\delta$ for the case $\Omega_{i,non}^\delta \cap \partial\Omega = \emptyset$ since all the boundary nodal values of $\Omega_{i,non}^\delta$ belong to $W_{i,in}^{\Gamma^\delta}$ and therefore have nodal values equal to one. For the case $\Omega_{i,non}^\delta \cap \partial\Omega \neq \emptyset$, we have chosen to define $\phi^i(\Omega_{i,non}^\delta)$ as the discrete harmonic extension with boundary nodal values equal to one on $W_{i,in}^{\Gamma^\delta}$ and equal to zero at $\bar{\Omega}_{i,non}^\delta \cap \partial\Omega$; note however we do not require that $\tilde{\mathcal{V}}_0^\delta$ be discrete harmonic on $\Omega_{i,non}^\delta$. If we had chosen ϕ^i equal to one at all nodes of $\Omega_{i,non}^\delta$ also for the $\Omega_{i,non}^\delta \cap \partial\Omega \neq \emptyset$ case, ϕ^i would have a jump from one to zero on the neighboring elements of $\partial\Omega$. This jump would give lower bounds that depend on the factor h/H , and such bound would be poor if the overlap is very small. Another possibility to avoid the discrete harmonicity of ϕ^i on $\Omega_{i,non}^\delta$ in the $\Omega_{i,non}^\delta \cap \partial\Omega \neq \emptyset$ case would be the use of the boundary layer technique developed in [21]. We note however that the bounds of Theorem 5.1 would remain the same as well as the its analysis, with some minor modifications.

The coarse space $\tilde{\mathcal{V}}_0^\delta$ is simply the space spanned by all linear combinations of the coarse basis functions $\phi^i, i = 1, \dots, N$. We define $\tilde{P}_0^\delta : \mathcal{V} \rightarrow \tilde{\mathcal{V}}_0^\delta$ as the operator such that, for any $u \in \mathcal{V}$

$$a(\tilde{P}_0^\delta u, v) = a(u, v), \quad \forall v \in \tilde{\mathcal{V}}_0^\delta.$$

A two-level additive version of RASHO can now be introduced with the operator

$$(4.2) \quad \tilde{P}_C^\delta = \sum_{i=0}^N \tilde{P}_i^\delta.$$

The convergence properties of this two-level algorithm will be studied in the next section. To describe the computational aspects of the coarse problem, we rewrite the above definitions in matrix notations. Recall that n is the total number of nodes in W , N is the total number of subdomains, and ϕ^i is the coarse basis function. We write the fine to coarse restriction operator as an $N \times n$ matrix

$$\left(\tilde{R}_0 \right)_{N \times n} = (\phi^i(x_k))_{i=1, N; k=1, n}.$$

The matrix form of the coarse projection operator \tilde{P}_0^δ is

$$(4.3) \quad \tilde{P}_0^\delta = \tilde{R}_0^T \tilde{A}_0^{-1} \tilde{R}_0 A,$$

where $\tilde{A}_0 = \tilde{R}_0 A \tilde{R}_0^T$ is an $N \times N$ matrix.

We remark that \tilde{A}_0 is more sparse than coarse space matrices that appear in other methods such as Neumann-Neumann or FETI type algorithms [12, 13, 18, 23], since only connections with the neighboring subdomains appear in the stencils associated to a coarse basis function. Another feature of this coarse space problem is that the computation of the right-hand side, i.e. $\tilde{R}_0 A u$, for some u , can be done inside each Ω_i^δ ; this is a clear advantage over regular coarse spaces.

The two-level additive algorithm (4.2) is easy to code, but the performance isn't as good as expected. Some examples are given in the numerical experiments section of this paper. We next introduce another two-level algorithm – a hybrid Schwarz operator (see [19]) with the error propagation operator given by

$$(4.4) \quad \left(I - \tilde{P}_0^\delta \right) \left(I - \sum_{i=1}^N \tilde{P}_i^\delta \right) \left(I - \tilde{P}_0^\delta \right).$$

This is a symmetric operator with which we can work essentially without any extra cost, since when forming powers of the operator (4.4) on building the Krylov space on the PCG, we can use the fact that $I - \tilde{P}_0^\delta$ is a projection, and therefore $(I - \tilde{P}_0^\delta)^2 = I - \tilde{P}_0^\delta$. Subtracting the operator (4.4) from the identity operator I , we obtain the operator

$$(4.5) \quad \tilde{P}_{hyb}^\delta = \tilde{P}_0^\delta + \left(I - \tilde{P}_0^\delta\right) \left(\sum_{i=1}^N \tilde{P}_i^\delta\right) \left(I - \tilde{P}_0^\delta\right).$$

The spectral properties of \tilde{P}_{hyb}^δ will be studied in the next section. Some numerical results obtained using the additive and the hybrid two-level methods will be presented in the numerical experiments section of the paper, and they will both be compared with the single level method.

5. Theoretical analysis. The algorithm presented in the previous section is applicable for general sparse, symmetric positive definite linear systems. The notions of subdomains, harmonic overlaps, the classification of the nodal points, etc, can all be defined in terms of the graph of the sparse matrix. In this section we provide a nearly optimal estimate for a Poisson equation discretized with a piecewise linear finite element method. We estimate the condition number of the RASHO operators \tilde{P}^δ and \tilde{P}_C^δ in terms of the fine mesh size h , the subdomain size H , and the overlapping factor δ . We shall follow the abstract additive Schwarz theory [24]:

Lemma 5.1. *Suppose the following assumptions hold:*

- i) *There exists a constant C_0 such that for any $u \in \tilde{\mathcal{V}}^\delta$ there exists a decomposition*

$$u = \sum_{i=0}^N u_i,$$

where $u_i \in \tilde{\mathcal{V}}_i^\delta$, and

$$\sum_{i=0}^N |u_i|_{H^1(\Omega)}^2 \leq C_0^2 |u|_{H^1(\Omega)}^2.$$

- ii) *There exist constants ϵ_{ij} , $i, j = 1, \dots, N$ such that*

$$a(u_i, u_j) \leq \epsilon_{ij} a(u_i, u_i)^{1/2} a(u_j, u_j)^{1/2}, \quad \forall u_i \in \tilde{\mathcal{V}}_i^\delta, \quad \forall u_j \in \tilde{\mathcal{V}}_j^\delta.$$

Then, \tilde{P}_C^δ is invertible, symmetric; i.e., $a(\tilde{P}_C^\delta u, v) = a(u, \tilde{P}_C^\delta v)$,

$$(5.1) \quad C_0^{-2} a(u, u) \leq a(\tilde{P}_C^\delta u, u) \leq (\rho(\mathcal{E}) + 1) a(u, u), \quad \forall u \in \tilde{\mathcal{V}}^\delta.$$

Here $\rho(\mathcal{E})$ is the spectral radius of \mathcal{E} , which is a $(N) \times (N)$ matrix made of $\{\epsilon_{ij}\}$.

It is trivial to see that $\rho(\mathcal{E}) \leq C$. So our focus in the rest of the section is in bounding C_0 . For the case of the single level RASHO, the lemma above can be modified by replacing $u = \sum_{i=0}^N u_i$, \tilde{P}_C^δ , and $(\rho(\mathcal{E}) + 1)$ above to $u = \sum_{i=1}^N u_i$, \tilde{P}^δ , and $\rho(\mathcal{E})$, respectively.

To analyze the hybrid algorithm we use a result due to Mandel (Lemma 3.2 [19]) which in our context is given by

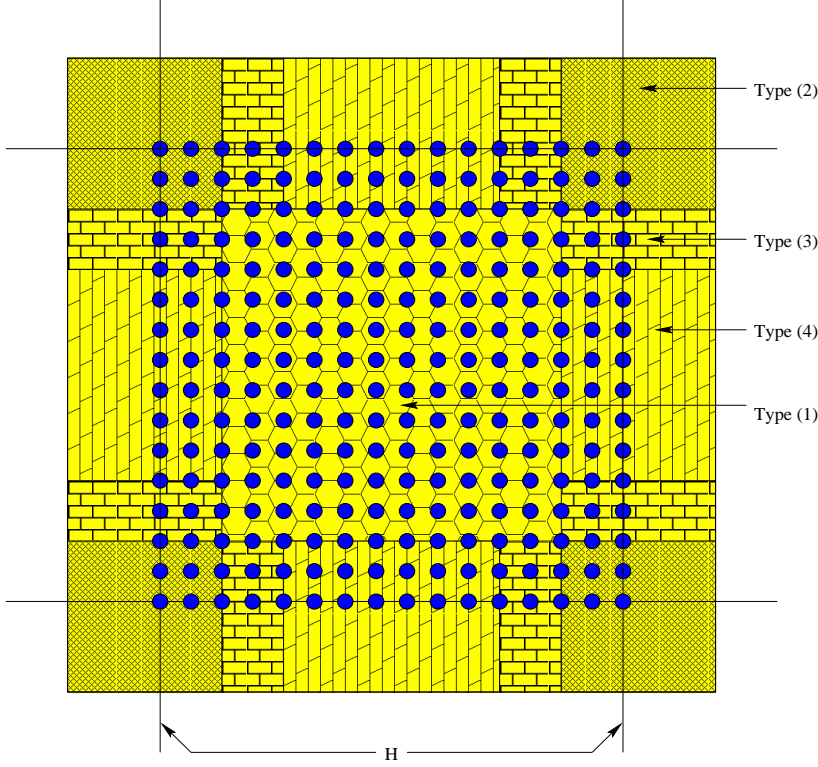


FIG. 5.1. The partition of Ω_i^δ into the union of four types of subregions. This is a ‘floating’ subdomain with $\delta = 2$. The collection of “•” forms the set W_i^0 .

Lemma 5.2. The extreme eigenvalues of \tilde{P}_{hyb}^δ , \tilde{P}_C^δ , and \tilde{P}^δ satisfy

$$\lambda_{min}(\tilde{P}_{hyb}^\delta) \geq \lambda_{min}(\tilde{P}_C^\delta) \quad \text{and} \quad \lambda_{max}(\tilde{P}_{hyb}^\delta) \leq \lambda_{max}(\tilde{P}^\delta).$$

5.1. The partition of unity and a comparison function. The construction of a partition of unity is one of the key steps in an additive Schwarz analysis. Consider $\phi^i(x)$ defined in (4.1). It is easy to see that $\{\phi^i(x), i = 1, \dots, N\}$ restricted to W^{Γ^δ} forms a partition of unit.

In addition to $\phi^i(x)$, we also need to construct a *comparison function* $\theta_i(x)$ for each subdomain Ω_i^δ . Comparison functions, or barrier functions, are very useful for many Schwarz algorithms, such as these on non-matching grids [6]. We will show that, even though $\theta_i(x) \in \mathcal{V}_i^\delta$, not in $\tilde{\mathcal{V}}_i^\delta$ as we wished, it can still be used to bound functions in $\tilde{\mathcal{V}}_i^\delta$. Both $\theta_i(x)$ and $\phi^i(x)$ depend on the overlapping factor δ . Because $\phi^i(x)$ is discrete harmonic at $W_{i,ovl}^\delta \cup W_{i,non}^\delta$, and identical to θ_i at the remaining nodes, we have

$$a(\phi^i, \phi^i) \leq a(\theta_i, \theta_i).$$

To construct the function $\theta_i(x)$, we first consider the case when Ω_i^0 is a floating square subdomain. “Floating” refers to the fact that the subdomain doesn’t touch the

boundary $\partial\Omega$. The extension to cases when Ω_i^δ touches the boundary is simple and we will comment on it later. To further simplify our arguments, we assume that Ω_i^δ and its neighboring extended subdomains Ω_j^δ are squares of the same size; i.e. sides length equal to $H + 2(\delta + 1)h$. This assumption is equivalent to that Ω^R has size H and δ levels of overlap is applied; see Fig. 5.1. And we also assume the overlap is not too large; for the analysis given below δh no larger than $H/4$ is enough. Our techniques can be modified to consider larger overlaps and more complex subdomains, although too large of an overlap has little practical value.

Roughly speaking, $\theta_i(x)$ is equal to $\phi^i(x)$ on $W \setminus W_{i,ovl}^\delta$. On the overlapping region $W_{i,ovl}^\delta$ we need to define $\theta_i(x)$ carefully so that we can control its energy in the semi H^1 norm. For this purpose, we decompose Ω_i^δ into subregions of four types (see Fig. 5.1): $\Omega_{i,non}^\delta$ (**Type (1)**), $\Omega_i^{\delta\delta}$ (**Type (2)**), $\Omega_i^{\delta H}$ (**Type(3)**), and $\Omega_i^{\delta\delta}$ (**Type (4)**), and define $\theta_i(x)$ on each piece of the subregion separately.

Type (1): The first subregion is $\Omega_{i,non}^\delta$, which a square with sides of size $H - 2\delta h$.

Type (2): The second subregion $\Omega_i^{\delta\delta}$ is the area where Ω_i^δ overlaps simultaneously with three neighbors Ω_j^δ . $\Omega_i^{\delta\delta}$ therefore represents the union of the four corner pieces of Ω_i^δ ; i.e. four squares with sides of size $(2\delta + 1)h$.

Type (3) and (4): The area where Ω_i^δ overlaps only one neighbor are four rectangles of size $H - 2\delta h \times (2\delta + 1)h$. We further partition each of the four rectangles into three smaller rectangles; i.e. two of them are of $\Omega_i^{\delta\delta}$ type and one of them of $\Omega_i^{\delta H}$ type. For instance, without loss of generality, let us consider the intersection of Ω_i^δ with its right neighbor Ω_j^δ , excluding the corner parts. In this case, the subregion to be partitioned is a rectangle of size $(2\delta + 1)h$ in the x direction and $H - 2\delta h$ in the y direction. The partition of this rectangles gives two smaller rectangles of $\Omega_i^{\delta\delta}$ type with dimensions $2(\delta + 1)h \times \delta h$ and each one has an edge in common with a square of $\Omega_i^{\delta\delta}$ type. We denote them as transition subregions because they are placed between a corner type subregion $\Omega_i^{\delta\delta}$ and a face type subregion $\Omega_i^{\delta H}$. The $\Omega_i^{\delta H}$ face type subregions are the smaller rectangles that are placed between the two smaller rectangles of $\Omega_i^{\delta\delta}$ type. $\Omega_i^{\delta H}$ face type regions are of size $(2\delta + 1)h$ by $H - 4\delta h$.

For any node x belonging to a **Type (1)** region $\Omega_{i,non}^\delta$, we define $\theta_i(x)$ to be equal to one; i.e., equal to $\phi^i(x)$. Therefore

$$|\phi^i(x)|_{H^1(\Omega_{i,non}^\delta)}^2 = |\theta_i(x)|_{H^1(\Omega_{i,non}^\delta)}^2 = 0.$$

We next define $\theta_i(x)$, node by node, in $\Omega_{i,ovl}^\delta$, which is the union of corner, transition and face type regions defined above.

For a **Type (2)** region $\Omega_i^{\delta\delta}$. Let Q be such a square with vertices $V_1 = (a, b)$, $V_2 = (a + (2\delta + 1)h, b)$, $V_3 = (a, b + (2\delta + 1)h)$, and $V_4 = (a + (2\delta + 1)h, b + (2\delta + 1)h)$. We assume that V_1, V_2 , and V_4 belong to $\partial\Omega_i^\delta$. In other words, Q is located on the southeast corner of Ω_i^δ . Let us also introduce another square region \tilde{Q} , with vertices $V_3 = (a, b + (2\delta + 1)h)$, $\tilde{V}_1 = (a, b + \delta h)$, $\tilde{V}_2 = (a + (\delta + 1)h, b + \delta h)$, and $\tilde{V}_4 = (a + (\delta + 1)h, b + (2\delta + 1)h)$. Note that \tilde{Q} is contained in Q , with V_3 as the common vertex. To define $\theta_i(x)$ on Q , we set $\theta_i(V_3) = 1$, $\theta_i(\tilde{V}_1) = 0$, $\theta_i(\tilde{V}_2) = 0$, $\theta_i(\tilde{V}_4) = 0$. At the remaining nodes x on the edges $\tilde{V}_1\tilde{V}_2$ and $\tilde{V}_2\tilde{V}_4$ we set $\theta_i(x) = 0$, and on the edges $V_3\tilde{V}_1$ and $V_3\tilde{V}_4$ we set $\theta_i(x) = 1$. For nodes on $Q \setminus \tilde{Q}$ we set $\theta_i(x) = 0$. It remains only to define $\theta_i(x)$ for nodes x in the interior of \tilde{Q} . To define $\theta_i(x)$ there we use a well-known cutoff function technique, such as the one introduced in Lemma 4.4 of [10] but for two-dimensional square regions. An illustrative picture of $\theta_i(x)$ in a

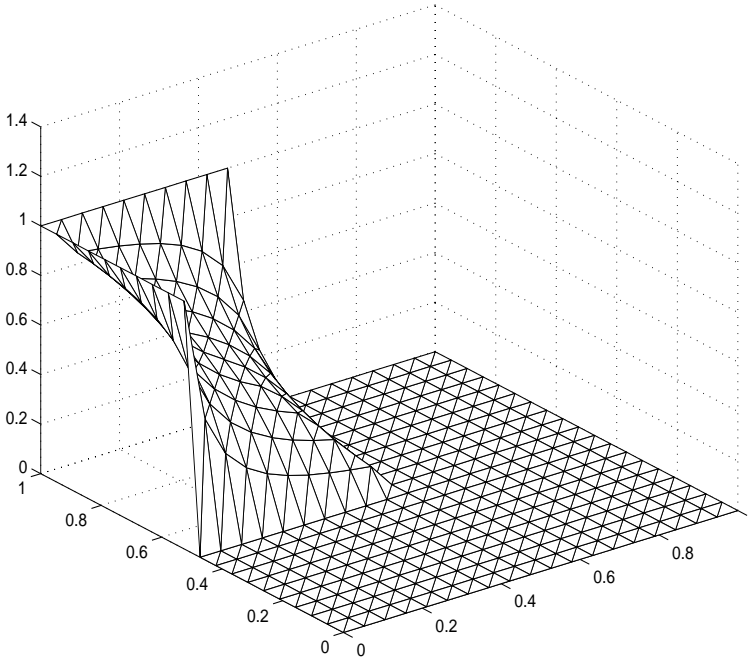


FIG. 5.2. An illustrative picture of $\theta_i(x)$ in a typical region $\Omega_i^{\delta\delta}$.

typical region $\Omega_i^{\delta\delta}$ is shown in Fig 5.2. For the completeness of this paper, we include the construction below. Let C be the center of the square \tilde{Q} . The construction of $\theta_i(x)$ is defined by the following steps:

- (1) Define $\theta_i(V_3) = 1$, $\theta_i(\tilde{V}_2) = 0$, $\theta_i(\tilde{V}_1) = 0$ and $\theta_i(\tilde{V}_4) = 0$.
- (2) For a point P that belongs to the segments $V_3\tilde{V}_4$ or $V_3\tilde{V}_1$, define $\theta_i(P) = 1$. For a point P that belongs to the segments $\tilde{V}_4\tilde{V}_2$ or $\tilde{V}_1\tilde{V}_2$, define $\theta_i(P) = 0$.
- (3) For a point Y that belongs to the line segment connecting C to V_3 , define $\theta_i(Y)$ by linear interpolation between values $\theta_i(C) = 1/2$ and $\theta_i(V_3) = 1$. For a point Y that belongs to the line segment connecting C to \tilde{V}_2 , define $\theta_i(Y)$ by linear interpolation between values $\theta_i(C) = 1/2$ and $\theta_i(\tilde{V}_2) = 0$.
- (4) For a point S that belongs to a line segment connecting a point Y to a vertex \tilde{V}_1 or \tilde{V}_4 , define $\theta_i(S) = \theta_i(Y)$.
- (5) Note that the θ_i is defined everywhere on $\tilde{Q} \cup \partial\tilde{Q}$. θ_i is continuous everywhere except at the points \tilde{V}_1 and \tilde{V}_4 . We redefine θ_i as the continuous piecewise linear finite element function given by the standard pointwise interpolation.

The most important observation of the construction of $\theta_i(x)$ inside \tilde{Q} is that $|\nabla\theta_i(x)| \leq C/r$ near \tilde{V}_1 or \tilde{V}_4 . Here r is the distance of x to \tilde{V}_1 or \tilde{V}_4 . Therefore, we obtain (see [10] and [23])

$$|\theta_i(x)|_{H^1(Q)}^2 = |\theta_i(x)|_{H^1(\tilde{Q})}^2 \leq C \left(1 + \log \left(\frac{(\delta+1)h}{h} \right) \right) = C(1 + \log(\delta+1)).$$

Since inside of Ω_i^δ there are four of those squares we obtain

$$|\theta_i(x)|_{H^1(\Omega_i^{\delta s})}^2 \leq C(1 + \log(\delta + 1)).$$

Type (3) regions consist of transition type rectangles. Let us consider one of them and denote it by T , which we assume has vertices at $V_3 = (a, b + (2\delta + 1)h)$, $V_4 = (a + (2\delta + 1)h, b + (2\delta + 1)h)$, $V_5 = (a, b + (3\delta + 1)h)$, and $V_6 = (a + (2\delta + 1)h, b + (3\delta + 1)h)$. Note that T stands on the top of the square Q introduced above and has the common edge V_3V_4 . We define $\theta_i(x)$ over the edge V_3V_4 to be equal to $\phi^i(x)$. Over the edge V_3V_5 , we set $\theta_i(x) = 1$. Over the edge V_4V_6 , we set $\theta_i(x) = 0$. And over the edge V_5V_6 we let $\theta_i(x)$ decrease linearly from the value 1 to 0. What remains is to define $\theta_i(x)$ inside T . Let us define the nodes $V_l = (a + \delta h, b + (2\delta + 1)h)$ and $V_r = (a + (\delta + 1)h, b + (2\delta + 1)h)$, which is the same as the node \tilde{V}_4 used in the description of **Type (2)** regions. The nodes V_l and V_r are exactly the places on the edge V_3V_4 where $\phi^i(x)$ jumps from 1 to 0. On the triangle $V_3V_lV_5$ we set $\theta_i(x) = 1$. On the triangle $V_rV_4V_6$ we set $\theta_i(x) = 0$. On the region $V_lV_rV_6V_5$, we let $\theta_i(x)$ decrease linearly in the x direction from the value 1 to 0. We note that next to the nodes V_lV_r , $\theta_i(x)$ has a singular behavior similar to $|\nabla\theta_i(x)| \leq C/r$ where r is the distance from x to the line V_lV_r . Similarly, we have

$$|\theta_i(x)|_{H^1(T)}^2 \leq C(1 + \log(\delta + 1)).$$

Since there are eight rectangles of **Type (3)** inside $\Omega_i^{\delta\bar{\delta}}$, we obtain

$$|\theta_i(x)|_{H^1(\Omega_i^{\delta\bar{\delta}})}^2 \leq C(1 + \log(\delta + 1)).$$

Type (4) regions are rectangles of face type. Let R be one of them, and we assume that the vertices are given by $V_5 = (a, b + (3\delta + 1)h)$, $V_6 = (a + (2\delta + 1)h, b + (3\delta + 1)h)$, $V_7 = (a, b + H - (\delta - 1)h)$, and $V_8 = (a + (2\delta + 1)h, b + H - (\delta - 1)h)$. Note that R is on the top of the rectangle T defined above and its height is $H - 4\delta h$. The vertices V_6 and V_8 are the vertices that belong to $\partial\Omega_i^\delta$. We define $\theta_i(x) = 1$ if x is on the edge V_5V_7 , and equals zero if x is on the edge V_6V_8 , and linear in the x direction for the remaining points. We obtain then

$$|\theta_i(x)|_{H^1(R)}^2 \leq \frac{H - 4\delta h}{(2\delta + 1)h}.$$

Since there are four of those rectangles inside $\Omega_i^{\delta H}$, we obtain

$$|\theta_i(x)|_{H^1(\Omega_i^{\delta H})}^2 \leq C \frac{H - 4\delta h}{(2\delta + 1)h} \leq C \frac{H}{(2\delta + 1)h}.$$

For the cases in which Ω_i^0 touches the boundary $\partial\Omega$, the analysis needs to be modified slightly. The first modification is because the shape of the overlapping region changes slightly, i.e. the longer side is shorter. It is easy to see that we get similar bounds as before. The other modification is because ϕ^i on $\Omega_{i,non}^\delta$ is not identically equal to one and therefore the corresponding energy is not necessarily zero. For this case we can design θ_i similarly and obtain

$$|\theta_i(x)|_{H^1(\Omega_{i,non}^\delta)}^2 \leq C \left(1 + \log \left(\frac{H}{h} \right) \right).$$

Putting all pieces of $\theta_i(x)$ together, we see that $\theta_i(x) \in \mathcal{V}_i^\delta$ and it is equal to $\phi^i(x)$ on W^{Γ^δ} . Adding all the estimates on subregions of four types, we arrive at the following lemma.

Lemma 5.3. *For $i = 1, \dots, N$, hold $\theta_i(x) \in \mathcal{V}_i^\delta$ and $\phi^i(x) \in \tilde{\mathcal{V}}_i^\delta$ the following*

- (1) $|\phi^i|_{H^1(\Omega_i^\delta)}^2 \leq |\theta_i|_{H^1(\Omega_i^\delta)}^2$.
- (2)

$$|\theta_i|_{H^1(\Omega_i^\delta \setminus \Omega_{i,non}^\delta)}^2 \leq C \left(1 + \log(\delta + 1) + \frac{H}{(2\delta + 1)h} \right).$$

(3) if $\Omega_{i,non}^\delta \cap \partial\Omega = \emptyset$ then $|\theta_i|_{H^1(\Omega_{i,non}^\delta)}^2 = 0$.

(4) if $\Omega_{i,non}^\delta \cap \partial\Omega \neq \emptyset$ then

$$|\theta_i|_{H^1(\Omega_{i,non}^\delta)}^2 \leq C \left(1 + \log \left(\frac{H}{h} \right) \right).$$

Here $C > 0$ is independent of the parameters h , H and δ .

5.2. A bounded partition lemma. To obtain the parameter C_0 of Assumption i) of the abstract additive Schwarz theory, see Lemma 5.1, we construct a decomposition of $\tilde{\mathcal{V}}^\delta$ and prove its boundedness below.

Lemma 5.4. *There exists a constant $C > 0$, independent of h , H , and δ , such that for any $u \in \tilde{\mathcal{V}}^\delta$, there exist $v_i \in \tilde{\mathcal{V}}_i^\delta$, such that*

$$(5.2) \quad u = \sum_{i=0}^N v_i,$$

and

$$(5.3) \quad \sum_{i=0}^N |v_i|_{H^1(\Omega)}^2 \leq C \left(\left(\frac{H}{(2\delta + 1)h} \right) |u|_{H^1(\Omega)}^2 + C(1 + \log(\delta + 1)) \left(1 + \log \left(\frac{H}{h} \right) \right) |u|_{H^1(\Omega)}^2 \right).$$

In addition, there exist $u_i \in \tilde{\mathcal{V}}_i^\delta$, such that

$$(5.4) \quad u = \sum_{i=1}^N u_i,$$

and

$$(5.5) \quad \sum_{i=1}^N |u_i|_{H^1(\Omega)}^2 \leq C(1 + \log(\delta + 1)) \left(1 + \log \left(\frac{H}{h} \right) \right) |u|_{H^1(\Omega)}^2 + C \frac{1}{H^2} \left(1 + \log(\delta + 1) + \frac{H}{(2\delta + 1)h} \right) |u|_{H^1(\Omega)}^2.$$

Proof. We first construct the decomposition (5.4). For any given $u \in \widetilde{\mathcal{V}}^\delta$, we define $u_i \in \widetilde{\mathcal{V}}_i^\delta$ as

$$u_i(x_k) = \begin{cases} u(x_k) & \text{if } x_k \in W_{i,in}^\delta \\ \text{discrete harmonic} & \text{if } x_k \in W_{i,ovl}^\delta \\ 0 & \text{if } x_k \in W \setminus \widetilde{W}_i^\delta. \end{cases}$$

It is easy to see (5.4) holds. We next construct the decomposition (5.2). For $i = 1, \dots, N$, let us define $v_i \in \widetilde{\mathcal{V}}_i^\delta$ by

$$v_i = u_i - \bar{u}_i \phi^i \in \widetilde{\mathcal{V}}_i^\delta,$$

where

$$\bar{u}_i = \frac{1}{|\Omega_i^\delta|} \int_{\Omega_i^\delta} u dx$$

is the average of u on the extended region Ω_i^δ . Here $|\Omega_i^\delta|$ is the area of the region Ω_i^δ . We also define

$$v_0 = \sum_{i=1}^N \bar{u}_i \phi^i.$$

It is easy to see (5.2) holds.

The next step is to bound $\sum_{i=1}^N |v_i|_{H^1(\Omega)}^2$. To bound each term $|v_i|_{H^1(\Omega)}^2, i = 1, \dots, N$, we use $\theta_i(x), i = 1, \dots, N$, introduced before. Consider $\tilde{v}_i \in \mathcal{V}_i^\delta$ defined as follows

$$\tilde{v}_i(x) = I_h(\theta_i(x)(u(x) - \bar{u}_i)).$$

Note that $\tilde{v}_i(x)$ is equal to $v_i(x)$ on $W_i^{\Gamma^\delta}$, and on $\partial\Omega_i^\delta$. On $\Omega_{i,ovl}^\delta$, v_i is discrete harmonic. Therefore, we have

$$|v_i|_{H^1(\Omega_{i,ovl}^\delta)}^2 \leq |\tilde{v}_i|_{H^1(\Omega_{i,ovl}^\delta)}^2.$$

In addition, $v_i(x)$ is identical to \tilde{v}_i on $\Omega_{i,non}^\delta$ whenever $\Omega_{i,non}^\delta$ does not touch $\partial\Omega$. For such cases, we next devote the proof to the estimate of $|\tilde{v}_i|_{H^1(\Omega_i^\delta)}^2$ in terms of $|u|_{H^1(\Omega_i^\delta)}^2$. The estimate of $|v_i|_{H^1(\Omega_{i,non}^\delta)}^2$ for the case in which $\Omega_{i,non}^\delta$ does not touch $\partial\Omega$ is done afterwards in (5.10).

Let K be an element of Ω_i^δ and let us denote $w_i = u - \bar{u}_i$ then

$$(5.6) \quad |\tilde{v}_i|_{H^1(K)}^2 = |I_h(\theta_i w_i)|_{H^1(K)}^2 \leq 2|\bar{\theta}_i w_i|_{H^1(K)}^2 + 2|I_h((\bar{\theta}_i - \theta_i)w_i)|_{H^1(K)}^2.$$

Here, $\bar{\theta}_i$ is the average of θ_i on K , and I_h is the standard pointwise interpolation. To estimate the first part of (5.6) we use the fact that $|\bar{\theta}_i| \leq 1$, to obtain

$$|\bar{\theta}_i w_i|_{H^1(K)}^2 = |\bar{\theta}_i(u - \bar{u}_i)|_{H^1(K)}^2 \leq |u - \bar{u}_i|_{H^1(K)}^2 = |u|_{H^1(K)}^2.$$

The last equality comes from the fact that \bar{u}_i is a constant. For the second part of (5.6), according to an inverse inequality we have

$$(5.7) \quad |I_h((\bar{\theta}_i - \theta_i)w_i)|_{H^1(K)}^2 \leq C \frac{1}{h^2} \|I_h((\bar{\theta}_i - \theta_i)w_i)\|_{L^2(K)}^2.$$

To obtain the bound for the right-hand side of (5.7), we consider the element K in four different situations corresponding to the four types of subregions into which the subregion Ω_i^δ is split i.e., $\Omega_{i,non}^\delta$, $\Omega_i^{\delta H}$, $\Omega_i^{\delta\delta}$ and $\Omega_i^{\delta\delta}$.

The proof for the cases $K \subset \Omega_i^{\delta H}$ and $K \subset \Omega_i^{\delta\delta}$ are nearly the same, so we only consider one of them here. For $K \subset \Omega_i^{\delta H}$, since

$$\|\bar{\theta}_i - \theta_i\|_{L^\infty(K)} \leq C \left(\frac{h}{(2\delta + 1)h} \right)^2,$$

we obtain

$$\frac{1}{h^2} \|I_h((\bar{\theta}_i - \theta_i)w_i)\|_{L^2(K)}^2 \leq C \frac{1}{((2\delta + 1)h)^2} \|w_i\|_{L^2(K)}^2.$$

Applying a technique developed in Dryja and Widlund [11], we obtain

$$(5.8) \quad \begin{aligned} & \frac{1}{((2\delta + 1)h)^2} \|w_i\|_{L^2(\Omega_i^{\delta H})}^2 \leq \\ & C \left(\frac{H}{(2\delta + 1)h} |w_i|_{H^1(\Omega_i^\delta)}^2 + \frac{1}{H((2\delta + 1)h)} \|w_i\|_{L^2(\Omega_i^\delta)}^2 \right). \end{aligned}$$

Using the fact $|w_i|_{H^1(\Omega_i^\delta)}^2 = |u|_{H^1(\Omega_i^\delta)}^2$ and a Friedrichs inequality

$$(5.9) \quad \|w_i\|_{L^2(\Omega_i^\delta)}^2 \leq CH^2 |u|_{H^1(\Omega_i^\delta)}^2.$$

Combining the estimates (5.8) and (5.9), we obtain

$$\frac{1}{((2\delta + 1)h)^2} \|w_i\|_{L^2(\Omega_i^{\delta H})}^2 \leq C \frac{H}{(2\delta + 1)h} |u|_{H^1(\Omega_i^\delta)}^2.$$

For the case when $K \subset \Omega_i^{\delta\delta}$, we use similar arguments as in Dryja, Smith and Widlund [10] to obtain

$$(5.10) \quad \sum_{K \in \Omega_i^{\delta\delta}} \frac{1}{h^2} \|I_h((\bar{\theta}_i - \theta_i)w_i)\|_{L^2(K)}^2 \leq \sum_{K \in \Omega_i^{\delta\delta}} C \frac{1}{r^2} \|w_i\|_{L^2(K)}^2,$$

where $ch \leq r \leq C((\delta + 1)h)$ is the distance to those ‘‘cut pieces’’. We have used here that $\theta_i(x)$ has the singular behavior C/r on $\Omega_i^{\delta\delta}$. We have then

$$(5.11) \quad \sum_{K \in \Omega_i^{\delta\delta}} \frac{1}{r^2} \|w_i\|_{L^2(K)}^2 \leq C \int_{ch}^{C(\delta+1)h} \int_{\alpha} r^{-2} r \|w_i\|_{L^\infty(\Omega_i^{\delta\delta})}^2 d\alpha dr$$

and

$$(5.12) \quad \|w_i\|_{L^\infty(\Omega_i^{\delta\delta})}^2 \leq C \left(1 + \log \left(\frac{H}{h} \right) \right) |u|_{H^1(\Omega_i^\delta)}^2.$$

For the inequality (5.12), we have used a well-known result (see Bramble [2])

$$\|u - \bar{u}_i\|_{L^\infty(\Omega_i^{\delta\delta})}^2 \leq \|u - \bar{u}_i\|_{L^\infty(\Omega_i^\delta)} \leq C \left(1 + \log \left(\frac{H}{h} \right) \right) \|u - \bar{u}_i\|_{H^1(\Omega_i^\delta)}^2$$

and that \bar{u}_i is the average of u on Ω_i^δ ; i.e., a Friedrichs inequality

$$\|u - \bar{u}_i\|_{H^1(\Omega_i^\delta)}^2 \leq C|u|_{H^1(\Omega_i^\delta)}^2.$$

Putting (5.11) and (5.12) together, we obtain

$$(5.13) \quad \sum_{K \in \Omega_i^{\delta h}} \frac{1}{r^2} \|w_i\|_{L^2(K)}^2 \leq C \left((1 + \log(\delta + 1)) \left(1 + \log\left(\frac{H}{h}\right) \right) \right) |u|_{H^1(\Omega_i^\delta)}^2.$$

For the case $K \subset \Omega_{i,non}^\delta$. If Ω_i^0 is a floating subdomain, which is to say that $\Omega_{i,non}^\delta$ does not touch $\partial\Omega$, then $\bar{\theta}_i - \theta_i$ is zero. If $\Omega_{i,non}^\delta$ touches the boundary $\partial\Omega$, then the estimate becomes

$$(5.14) \quad \begin{aligned} |v_i|_{H^1(\Omega_{i,non}^\delta)}^2 &\leq C \left(|u|_{H^1(\Omega_{i,non}^\delta)}^2 + |\bar{u}_i|^2 |\phi^i|_{H^1(\Omega_{i,non}^\delta)}^2 \right) \\ &\leq C \left(1 + \log\left(\frac{H}{h}\right) \right) |u|_{H^1(\Omega_i^\delta)}^2. \end{aligned}$$

Here we have used Lemma 5.3 and that for the cases $i \in \partial\Omega$, we can use a Poincaré inequality to obtain

$$(5.15) \quad \sum_{i \in \partial\Omega} |\bar{u}_i|^2 \leq C \sum_{i \in \partial\Omega} \frac{1}{H^2} \|u\|_{L^2(\Omega_i^\delta)}^2 \leq C \sum_{i \in \partial\Omega} |u|_{H^1(\Omega_i^\delta)}^2 \leq C |u|_{H^1(\Omega)}^2.$$

Here we have introduced the notation $i \in \partial\Omega$ to denote the subdomains Ω_i^0 that touch the boundary $\partial\Omega$ with a face.

Putting everything together we have shown that

$$(5.16) \quad \begin{aligned} \sum_{i=1}^N |v_i|_{H^1(\Omega)}^2 &\leq C \left(\left(\frac{H}{(2\delta + 1)h} \right) \right) |u|_{H^1(\Omega)}^2 + \\ &C(1 + \log(\delta + 1)) \left(1 + \log\left(\frac{H}{h}\right) \right) |u|_{H^1(\Omega)}^2. \end{aligned}$$

We remark that the bound (5.3) follows from (5.16). To see this, we use that $v_0 = u - \sum_i v_i$, triangular inequalities and (5.16) to obtain (5.3).

We now consider the bound for the one-level RASHO method; i.e., to bound $\sum_{i=1}^N u_i$. Note that

$$\sum_{i=1}^N u_i = \sum_{i=1}^N v_i + \sum_{i=1}^N \bar{u}_i \phi^i.$$

For the second sum above, we first use Lemma 5.3 to obtain

$$\sum_{i=1}^N |\bar{u}_i \phi^i|_{H^1(\Omega)}^2 \leq C \left(1 + \log\left(\frac{H}{h}\right) \right) \sum_{i \in \partial\Omega} |\bar{u}_i|^2 +$$

$$C \left(1 + \log(\delta + 1) + \frac{H}{(2\delta + 1)h} \right) \sum_{i=1}^N |\bar{u}_i|^2.$$

We then use Cauchy-Schwarz and Friedrichs inequalities to obtain

$$\begin{aligned} \sum_{i=1}^N |\bar{u}_i|^2 &= \sum_{i=1}^N \left(\frac{1}{|\Omega_i^\delta|} \int_{\Omega_i^\delta} u dx \right)^2 \leq C \sum_{i=1}^N \frac{1}{H^2} \|u\|_{L^2(\Omega_i^\delta)}^2 \\ &\leq C \frac{1}{H^2} \|u\|_{L^2(\Omega)}^2 \leq C \frac{1}{H^2} |u|_{H^1(\Omega)}^2. \end{aligned}$$

For the cases $i \in \partial\Omega$, we use (5.15). The inequality (5.5) then follows. \square

5.3. The main theorem. We state the main theorem of this paper here., The proof follows directly from all the abstract Schwarz theory given by Lemma 5.1, Lemma 5.2, and Lemma 5.4.

Theorem 5.1. *The RASHO operators \tilde{P}^δ , \tilde{P}_C^δ and \tilde{P}_{hyb}^δ are symmetric in the inner product $a(\cdot, \cdot)$, nonsingular, and bounded from below and above*

$$\begin{aligned} C_0^{-2} a(u, u) &\leq a(\tilde{P}_C^\delta u, u) \leq C_1 a(u, u) \quad \forall u \in \tilde{\mathcal{V}}^\delta, \\ \hat{C}_0^{-2} a(u, u) &\leq a(\tilde{P}^\delta u, u) \leq \hat{C}_1 a(u, u) \quad \forall u \in \tilde{\mathcal{V}}^\delta, \end{aligned}$$

and

$$\kappa(\tilde{P}_{hyb}^\delta) \leq \kappa(\tilde{P}_C^\delta).$$

Here

$$C_0^2 = C \left(\frac{H}{(2\delta + 1)h} + (1 + \log(\delta + 1)) \left(1 + \log\left(\frac{H}{h}\right) \right) \right),$$

and

$$\hat{C}_0^2 = C \left((1 + \log(\delta + 1)) \left(1 + \log\left(\frac{H}{h}\right) \right) + \frac{1}{H^2} \left(1 + \log(\delta + 1) + \frac{H}{(2\delta + 1)h} \right) \right).$$

The constants $C, C_1, \hat{C}_1 > 0$ are independent of h, H , and δ .

We remark that the corresponding convergence rate estimate for the regular one-level additive Schwarz methods [11], in terms of the constant \hat{C}_0 , is

$$\hat{C}_0^2 = C \left(1 + \frac{1}{H(2\delta + 1)h} \right),$$

and the two-level additive Schwarz method is

$$C_0^2 = C \left(1 + \frac{H}{\delta h} \right).$$

The lower bound \hat{C}_0^2 of the one-level RASHO algorithm is theoretically slightly worse than the lower bound of regular AS algorithm in the case of large overlap, but roughly the same for small overlap. For small overlap, the lower bounds of both algorithms behave like $O(H/h)$. When the overlap gets larger, the RASHO scheme starts to feel the factor $\log(H/h)$ and the performance gets worse than the additive version for

large overlap. On the other hand, the upper bound C_1 of RASHO is smaller than the upper bounds of AS. We can see this since $\tilde{\mathcal{V}}_k^\delta \subset \mathcal{V}_k^\delta, \forall k$, implies that the positive numbers ϵ_{ij} defined in Lemma 5.1 are smaller for RASHO than the corresponding ϵ_{ij} for AS. Consequently, the spectral radius \mathcal{E} of RASHO is smaller. Because C_1 of RASHO is smaller, the numerical performance of RASHO presented in the next section is better than that of AS for the practical cases. Similar considerations also apply to the two-level RASHO methods.

6. Numerical experiments. In this section, we present some numerical results for solving the Poisson's equation on the unit square with zero Dirichlet boundary conditions. We compare the performance of RASHO and AS preconditioned Conjugate Gradient methods in terms of the number of iterations and the condition numbers. We pay particular attention to the dependence on the number of subdomains and the size of overlap.

We first discuss a few implementation issues related to the new preconditioner. In order to apply the RASHO/CG method, it is necessary to force the solution to belong to $\tilde{\mathcal{V}}^\delta$. To do so, a pre-CG-computation is needed, and it is done through the formula (3.5). We note that $u = u^* - w \in \tilde{\mathcal{V}}^\delta$, see Lemma 3.1, and therefore, we can apply the regular PCG to the RASHO preconditioned system (3.9). The AS/CG is the classical additive Schwarz preconditioned CG as described in [8]. We note that in the case $\delta = 0$, i.e. $ovlp = h$, RASHO and AS are the same.

The stopping condition for CG is to reduce the initial residual by a factor of 10^{-6} . The exact solution of the equation is $u(x, y) = e^{5(x+y)} \sin(\pi x) \sin(\pi y)$. All subdomain problems are solved exactly. The iteration counts (iter), condition numbers (cond), maximum (max) and minimum (min) eigenvalues of the preconditioned matrix are summarized in tables 6.1-6.5.

From Table 6.1, Table 6.2, and Table 6.3, it is clear that for overlap not too large and for mesh not too small, which is the case of practical interest, the one-level RASHO/CG outperforms the classical one-level AS/CG in terms of the iteration counts and condition numbers. In this case of small the condition number of RASHO is almost twice smaller than AS. This is an important result since it is easy to modify a (parallel) one-level AS/CG code to obtain a one-level RASHO/CG implementation. Although we do not have any parallel results to report here, we are confident to predict that RASHO/CG would be even better than AS/CG on a parallel computer with distributed memory since much less communications are required. Also the local solvers in RASHO are slightly cheaper since the local solvers have slightly smaller numbers of unknowns than for the regular AS. From Table 6.4 we show that both the two-level hybrid and additive versions of RASHO attain scalability in terms of number of iterations when the number of subdomains becomes large; the hybrid version reaches the asymptotic behavior sooner than the additive version. The hybrid version is superior to the additive version since the number of iterations is much smaller. Finally, from Table 6.5 we show that larger overlap reduces dramatically the number of iterations.

TABLE 6.1

One-level RASHO and AS preconditioned CG for solving the Poisson's equation on a 128×128 mesh decomposed into $2 \times 2 = 4$ subdomains with overlap = *ovlp*. The AS/CG results are shown in (). The "+1" is for the preprocessing step needed for RASHO.

| <i>ovlp</i> | iter | cond | max | min |
|-------------|-----------|-------------|-------------|-----------------|
| <i>h</i> | 42 (42) | 129. (129.) | 1.98 (1.98) | 0.0154 (0.0154) |
| <i>3h</i> | 24+1 (28) | 48.4 (86.3) | 1.94 (4.00) | 0.0402 (0.0464) |
| <i>5h</i> | 20+1 (23) | 33.3 (51.8) | 1.91 (4.00) | 0.0574 (0.0773) |
| <i>7h</i> | 18+1 (20) | 27.2 (37.0) | 1.89 (4.00) | 0.0694 (0.1081) |

TABLE 6.2

One-level RASHO and AS preconditioned CG for solving the Poisson's equation on a $32 * DOM \times 32 * DOM$ mesh decomposed into $DOM \times DOM$ subdomains with overlap = $3h$, i.e. $\delta = 1$.

| $DOM \times DOM$ | iter | cond | max | min |
|------------------|-------------|--------------|-------------|-----------------|
| 2×2 | 19+1 (20) | 26.8 (43.7) | 1.89 (4.00) | 0.0708 (0.0916) |
| 4×4 | 39+1 (42) | 86.9 (145.) | 1.95 (4.00) | 0.0225 (0.0276) |
| 8×8 | 75+1 (78) | 328. (550.) | 1.97 (4.00) | 0.0060 (0.0073) |
| 16×16 | 147+1 (156) | 1295 (2168.) | 1.98 (4.00) | 0.0015 (0.0018) |

REFERENCES

- [1] S. BALAY, W. GROPP, L. MCINNES, AND B. SMITH, *The Portable Extensible Toolkit for Scientific Computing (PETSc)*, www.mcs.anl.gov/petsc, 2002.
- [2] J. BRAMBLE, *A second order finite difference analogue of the first biharmonic boundary value problem*, Numer. Math., 9 (1966), pp. 236-249.
- [3] S. BRENNER AND R. SCOTT, *The Mathematical Theory of Finite Element Methods*, Springer, 1994.
- [4] X.-C. CAI, M. CASARIN, F. ELLIOT, AND O. WIDLUND, *Overlapping Schwarz algorithms for solving Helmholtz's equation*, Contemporary Mathematics, 218 (1998), pp. 391-399.
- [5] X.-C. CAI, C. FARHAT, AND M. SARKIS, *A minimum overlap restricted additive Schwarz preconditioner and applications in 3D flow simulations*, Contemporary Mathematics, 218 (1998), pp. 479-485.
- [6] X.-C. CAI, T. MATHEW, AND M. SARKIS, *Maximum norm analysis of overlapping nonmatching grid discretizations of elliptic equations*, SIAM J. Numer. Anal., 37 (2000), pp. 1709-1728.
- [7] X.-C. CAI AND M. SARKIS, *A restricted additive Schwarz preconditioner for general sparse linear systems*, SIAM J. Sci. Comput., 21 (1999), pp. 792-797.
- [8] M. DRYJA AND O. WIDLUND, *An additive variant of the Schwarz alternating method for the case of many subregions*, Technical Report 339, also Ultracomputer Note 131, Department of Computer Science, Courant Institute, 1987.
- [9] M. DRYJA, M. SARKIS, AND O. WIDLUND, *Multilevel Schwarz methods for elliptic problems with discontinuous coefficients in three dimensions*, Numer. Math., 72 (1996), pp. 313-348.
- [10] M. DRYJA, B. SMITH, AND O. WIDLUND, *Schwarz analysis of iterative substructuring algorithms for elliptic problems in three dimensions*, SIAM J. Numer. Anal., 31 (1994), pp. 1662-1694.
- [11] M. DRYJA AND O. WIDLUND, *Domain decomposition algorithms with small overlap*, SIAM J. Sci. Comp., 15 (1994), pp. 604-620.
- [12] M. DRYJA AND O. WIDLUND, *Schwarz methods of Neumann-Neumann type for three-dimensional elliptic finite element problems*, Comm. Pure Appl. Math., 48 (1995), pp. 121-155.
- [13] C. FARHAT AND F. ROUX, *A method of finite element tearing and interconnecting and its parallel solution algorithm*, Int. J. Numer. Mech. Engrg., 32 (1991), pp. 1205-1227.
- [14] A. FROMMER AND D. SZYLD, *An algebraic convergence theory for restricted additive Schwarz methods using weighted max norms*, SIAM J. Numer. Anal., 39 (2001), pp. 463-479.

TABLE 6.3

One-level RASHO and AS preconditioned CG for solving the Poisson's equation on a $n \times n$ mesh decomposed into 4×4 subdomains with overlap = $3h$, i.e. $\delta = 1$.

| $DOM \times DOM$ | iter | cond | max | min |
|------------------|-----------|---------------|-------------|------------------|
| 64×64 | 30+1 (29) | 50.1 (72.2) | 1.91 (4.00) | 0.0382 (0.0554) |
| 128×128 | 39+1 (40) | 86.9 (145.) | 1.95 (4.00) | 0.0225 (0.0276) |
| 256×256 | 53+1 (56) | 159.9 (290.7) | 1.98 (4.00) | 0.0124 (0.0138) |
| 512×512 | 74+1 (77) | 305.6 (582.1) | 1.99 (4.00) | 0.0065 (0.00069) |

TABLE 6.4

Two-level hybrid and additive RASHO for solving the Poisson's equation on a $32 * DOM \times 32 * DOM$ mesh decomposed into $DOM \times DOM$ subdomains with overlap = $3h$, i.e. $\delta = 1$; The two-level additive RASHO results are shown in ().

| $DOM \times DOM$ | iter | cond | max | min |
|------------------|-------------|-------------|-------------|-----------------|
| 2×2 | 27+1 (30+1) | 24.2 (45.9) | 1.82 (2.90) | 0.0751 (0.0634) |
| 4×4 | 32+1 (46+1) | 27.2 (53.3) | 1.80 (2.93) | 0.0662 (0.0551) |
| 8×8 | 33+1 (52+1) | 28.4 (55.3) | 1.80 (2.94) | 0.0634 (0.0533) |
| 16×16 | 33+1 (52+1) | 28.8 (55.8) | 1.80 (2.94) | 0.0625 (0.0528) |

- [15] G. GOLUB AND C. VAN LOAN, *Matrix Computations*, The Johns Hopkins University Press, 1983.
- [16] W. GROPP, D. KAUSHIK, D. KEYES, AND B. SMITH, *Performance modeling and tuning of an unstructured mesh CFD application*, Proceedings of SC2000, IEEE Computer Society, 2000.
- [17] M. LESOINNE, M. SARKIS, U. HETMANIUK, AND C. FARHAT, *A linearized method for the frequency analysis of three-dimensional fluid/structure interaction problems in all flow regimes*, Comp. Meth. Appl. Mech. Eng., 190 (2001), pp. 3121-3146.
- [18] J. MANDEL, *Balancing domain decomposition*, Communications in Numerical Methods in Engineering, 9 (1993), pp. 233-241.
- [19] J. MANDEL, *Hybrid domain decomposition with unstructured subdomains*, Contemporary Mathematics, 157 (1994), pp. 103-112.
- [20] A. QUARTERONI AND A. VALLI, *Domain Decomposition Methods for Partial Differential Equations*, Oxford Science Publications, 1999.
- [21] M. SARKIS, *Partition of unity coarse spaces and Schwarz methods with harmonic overlap*, In the Proceedings of the Workshop in Domain Decomposition, ETH Zurich, June, 2001. Springer-Verlag in the LNCSE series, pp. 75-92. .
- [22] Y. SAAD AND M. SCHULTZ, *GMRES: A generalized minimum residual algorithm for solving nonsymmetric linear systems*, SIAM J. Sci. Stat. Comput., 7 (1986), pp. 856-869.
- [23] M. SARKIS, *Nonstandard coarse spaces and Schwarz methods for elliptic problems with discontinuous coefficients using non-conforming elements*, Numer. Math., 77 (1997), pp. 383-406.
- [24] B. SMITH, P. BJØRSTAD, AND W. GROPP, *Domain Decomposition: Parallel Multilevel Methods for Elliptic Partial Differential Equations*, Cambridge University Press, 1996.

TABLE 6.5

Two-level hybrid and additive RASHO CG for solving the Poisson's equation on a 512×512 mesh decomposed into $16 \times 16 = 256$ subdomains with overlap = $ovlp$. The two-level additive RASHO results are shown in ().

| $ovlp$ | iter | cond | max | min |
|--------|---------------|--------------|-------------|-----------------|
| h | 86 +1 (109+1) | 307 (275.7) | 1.96 (3.74) | 0.0064 (0.0136) |
| $3h$ | 44 +1 (68+1) | 48.0 (95.7) | 1.87 (2.98) | 0.0391 (0.0312) |
| $5h$ | 36 +1 (58+1) | 32.8 (70.1) | 1.83 (2.95) | 0.0558 (0.0421) |
| $7h$ | 31 +1 (53+1) | 27.3 (59.8) | 1.80 (2.93) | 0.0662 (0.0491) |